# Reuse 1 in WiMAX Networks with Beamforming

Masood Maqbool, Marceau Coupechoux, Philippe Godlewski

# Reuse 1 in WiMAX Networks with Beamforming

Masood Maqbool, Marceau Coupechoux, Philippe Godlewski
TELECOM ParisTech & CNRS LTCI
46, rue Barrault 75013 Paris, France
Email: {firstname.lastname}@telecom-paristech.fr

***Abstract*—In this paper, we examine the performance of adaptive beamforming in connection with three different subcarrier permutation schemes (PUSC, FUSC and AMC) in WiMAX cellular network with frequency reuse 1. Performance is evaluated in terms of radio quality parameters and system throughput. We show that organization of pilot subcarriers in PUSC Major groups has a pronounced effect on system performance while considering adaptive beamforming. Adaptive beamforming per PUSC group offers full resource utilization without need of coordination among base stations. Though FUSC is also a type of distributed subcarrier permutation, its performance in terms of outage probability is somewhat less than that of PUSC. We also show that because of lack of diversity, adjacent subcarrier permutation AMC has the least performance as far as outage phenonmenon is concerned. Results in this paper are based on Monte Carlo simulations performed in downlink.**

**Keywords: OFDMA, PUSC, FUSC, AMC, IEEE 802.16e, WiMAX, $SINR_{eff}$, MIC, beamforming.**

## I. Introduction

Mobile WiMAX, a broadband wireless access (BWA) technology, is based on IEEE standard 802.16-2005 [1]. Orthogonal frequency division multiple access (OFDMA) is a distinctive characteristic of physical layer of 802.16e based systems. The underlying technology for OFDMA based systems is orthogonal frequency division multiplexing (OFDM).

In OFDM, available spectrum is split into a number of parallel orthogonal narrowband subcarriers. These subcarriers are grouped together to form subchannels. The distribution of subcarriers to subchannels is done using three major permutation methods called: partial usage of subchannels (PUSC), full usage of subchannels (FUSC) and adaptive modulation and coding (AMC). The subcarriers in a subchannel for first two methods are distributed throughout the available spectrum while these are contiguous in case of AMC. Resources of an OFDMA system occupy place both in time (OFDM symbols) and frequency (subchannels) domains thus introducing both the time and frequency multiple access [2].

Adaptive beamforming technique is a key feature of mobile WiMAX. It does not only enhance the desired directional signal but also its narrow beamwidth reduces interference caused to the users in neighboring cells. Resultant increase in signal to interference-plus-noise ratio (SINR) offers higher capacity and lower outage probability, which is defined as the probability that a user does not achieve minimum SINR level required to connect to a service. Adaptive beamforming can be used with PUSC, FUSC and AMC (refer Tab.278 of [1]).

Network bandwidth is of high value for mobile network operators. It is always desired to get the maximum out of an available bandwidth by implementing frequency reuse 1 (network bandwidth being re-utilized in every sector see Fig. 1). However, with increased frequency reuse, radio quality of the users starts to deteriorate. Hence outage probability, which is defined as the probability that a user does not achieve minimum SINR level required to connect to a service probability, becomes more significant. To combat this problem, the conventional solution in existing literature is partial resource utilization or base station coordination to achieve frequency reuse 1.

Authors of [3] study the power gain, because of adaptive beamforming, of a IEEE 802.16e based system. Results presented by authors are based on measurements carried out in one sector of a cell with no consideration of interference. Measurements are carried out using an experimental adaptive beamforming system. Reference [4] discusses the performance of WiMAX network using beamforming in conjunction with space division multiple access (SDMA). The simulations are carried out for OFDM (not OFDMA). Hence frequency diversity, because of distributed subcarrier permutations, is not taken into account. In [5] and [6], author has analyzed the performance of beamforming capable IEEE 802.16e systems with AMC. Unlike distributed subcarrier permutations (PUSC and FUSC), subcarriers in an AMC subchannel are contiguous on frequency scale. Hence PUSC/FUSC offer more frequency diversity as compared to AMC. Suggested interference coordination technique allows reuse 1 at the cost of reduced resource utilization. In [7], we have carried out system level simulations for WiMAX networks. The analysis was focused on comparison of different frequency reuse patterns. Adaptive beamforming gain was also considered. We have shown that reuse 1 is possible with partial loading of subchannels.

In [8], however, we have shown that by employing beamforming per PUSC group, the antenna-plus-array gain can be

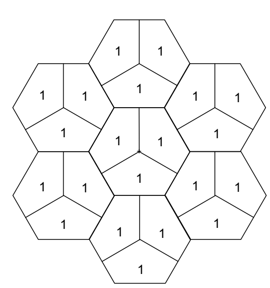

Fig. 1. Frequency Reuse Pattern 1x3x1.

diversified and as a result reuse 1 is possible without even partial loading of subchannels or base station coordination. In this paper, we extend the previous results by comparing the system performance with all three subcarrier permutation types (PUSC, FUSC and AMC). The performance is analyzed in terms of cell throughput, $SINR_{eff}$ and probability of outage. Monte Carlo simulations are carried out in downlink (DL) for this purpose.

Rest of the paper is organized as follows: section II gives an introductory account of subcarrier permutation types to be analyzed in this paper. Possibility of beamforming with different subcarrier permutation types is discussed in section III. SINR, beamforming, physical abstraction model MIC and simulator details are introduced in section IV. Simulation results have been presented in section V. Finally section VI discusses the conclusion of this analysis.

## II. Subcarrier Permutation Types

In this section, we present the salient features of subcarrier permutation with PUSC, FUSC and AMC in DL. A detailed account can be found in [9] where permutation method has been explained with the help of examples.

### A. Partial Usage of Subchannels (PUSC)

One slot of PUSC DL is two OFDM symbols by one subchannel while one PUSC DL subchannel comprises of 24 data subcarriers. Subchannels are built as follows:

1) The used subcarriers (data and pilots) are sequentially divided among a number of physical clusters such that each cluster carriers twelve data and two pilot subcarriers.
2) These physical clusters are permuted to form logical clusters using the renumbering formula on p. 530 in [1]. This process is called outer permutation. This permutation is characterized by a pseudo-random sequence and an offset called $DL\_PermBase$.
3) Logical clusters are combined together in six groups called the Major Groups. The even groups possess more logical clusters as compared to odd Major Groups. Throughout this paper, we shall refer these Major Groups as groups only.
4) The assignment of subcarriers to subchannels in a group is obtained by applying Eq. 111 of [1]. This process is known as inner permutation. The assignment in inner permutation is also controlled by $DL\_PermBase$. Pilot subcarriers are specific to each group. Since number of logical clusters is different in even and odd groups, the number of their respective subchannels is also different.

### B. Full Usage of Subchannels (FUSC)

The slot of in FUSC mode is one OFDM symbol by one subchannel. Since slot is in each permutation mode has same number of subcarriers, unlike in PUSC, the subchannel in FUSC comprises of 48 data subcarriers. Subcarriers are assigned to subchannels in following manner:

TABLE I
PUSC/FUSC/AMC parameters for 1024 FFT [1].

| **Subcarrier Permutation** | **Parameter** | **Value** |
|---|---|---|
| PUSC | No. of subchannels $N_{Sch}$ | 30 |
| | No. of subchannels per even group $N_e$ | 6 |
| | No. of subchannels per odd group $N_o$ | 4 |
| | No. of PUSC groups | 6 |
| | No. of total data subcarriers | 720 |
| | No. of total pilot subcarriers | 120 |
| FUSC | No. of subchannels $N_{Sch}$ | 16 |
| | No. of total data subcarriers | 768 |
| | No. of total pilot subcarriers | 82 |
| AMC | No. of subchannels $N_{Sch}$ | 48 |
| | No. of total data subcarriers | 768 |
| | No. of total pilot subcarriers | 96 |

1) Before subcarriers are assigned to subchannels, pilot subcarriers are first identified (subcarrier positions for pilot subcarriers are given in section 8.4.6.1.2.2 of [1]) and are separated from the rest. These pilot subcarriers are common to all subchannels.
2) In next step, the remaining subcarriers are divided among 48 groups.
3) Using Eq. 111 of [1], a particular subcarrier is picked up from each group and is assigned to a subchannel. Similar to inner permutation of PUSC, this assignment is also controlled by $DL\_PermBase$.

In PUSC and FUSC, by using different $DL\_PermBase$ in network cells, subcarriers of a given subchannel are not identical in adjacent cells. In this case, it has been shown in [10] and [11], that the above process is equivalent to choosing subcarriers using uniform random distribution on the entire bandwidth in every cell. During our simulations, we consider the same assumption.

### C. Adaptive Modulation and Coding (AMC)

In adjacent subcarrier permutation mode AMC, a slot is defined as $N_b$ bins $\times M$ OFDM symbols, where ($N_b \times M = 6$). All available subcarriers (data+pilot) are sequentially grouped into bins. A bin is composed of nine contiguous subcarriers such that eight are data and one is pilot subcarrier. Though not exclusively specified in [12] and [1], but in consistent with nomenclature of PUSC and FUSC, we call bits ensemble in a slot as subchannel. Out of possible combinations, we choose 2 bins $\times$ 3 OFDM symbols in our simulations.

## III. Subcarrier Permutation and Beamforming

Pilot subcarriers are used for channel estimation. In case of beamforming, dedicated pilots are required for each beam in the cell. For PUSC and FUSC, there is a common set of pilot subcarriers for a number of subchannels while in AMC mode, each subchannel has its own pilot subcarriers. Hence, the number of possible orthogonal beams in a cell (of cellular network) depends upon distribution of pilot subcarriers and hence subcarrier permutation type.

In PUSC, subchannels are put together in six groups. Each group has its own set of pilot subcarriers and hence, beamforming can be done per PUSC group. As subcarriers of a subchannel are chosen randomly, each subcarrier may experience the interference from the different beams of a given interfering cell. In this way, each subcarrier of a subchannel will have different interfering array-plus-antenna gain since the colliding subcarrier may belong to any of six interfering beams in neighboring cell. Details for beamforming with PUSC are given in [8].

Pilot subcarriers in FUSC are common to all subchannels hence only one orthogonal beam is possible in every cell. In contrast to PUSC, all subcarriers of a subchannel have same array-plus-antenna gain because of interfering beams.

When we consider AMC for beamforming, there can be as many orthogonal beams as many subchannel since every subchannel has its own pilot subcarriers. Due to similar assignment of subcarriers to subchannels in neighboring cells, all subcarriers will have same array-plus-antenna gain because of interfering beams. In addition, unlike PUSC and FUSC, since subcarriers of a subchannel are contiguous in AMC, no diversity gain is achieved.

## IV. Network and Interference Model

### A. Subcarrier SINR

SINR of a subcarrier $n$ is computed by the following formula:

$$SINR_n = \frac{P_{n,Tx} a_{n,Sh}^{(0)} a_{n,FF}^{(0)} \frac{K}{d^{(0)\alpha}}}{N_0 W_{Sc} + \sum_{b=1}^{B} P_{n,Tx} a_{n,Sh}^{(b)} a_{n,FF}^{(b)} \frac{K}{d^{(b)\alpha}} \delta_n^{(b)}} \quad (1)$$

where $P_{n,Tx}$ is the per subcarrier power, $a_{n,Sh}^{(0)}$ and $a_{n,FF}^{(0)}$ represent the shadowing (log-normal) and fast fading (Rician) factors for the signal received from serving BS respectively, $B$ is the number of interfering BS, $K$ is the path loss constant, $\alpha$ is the path loss exponent and $d^{(0)}$ is the distance between MS and serving BS. The terms with superscript $b$ are related to interfering BS. $W_{Sc}$ is the subcarrier frequency spacing, $N_0$ is the thermal noise density and $\delta_n^{(b)}$ is equal to 1 if interfering BS transmits on $n^{th}$ subcarrier and 0 otherwise.

### B. Effective SINR

Slot is the basic resource unit in an IEEE 802.16 based system. We compute $SINR_{eff}$ over the subcarriers of a slot. The physical abstraction model used for this purpose is MIC [10]. For computation of $SINR_{eff}$, log-normal shadowing is drawn randomly for a slot and is same for all subcarriers of a slot. For fast fading, Rice distribution has been considered in simulations. Rician K-factor has been referred from [13] (scenario C1). Since in PUSC and FUSC, subcarriers of a subchannel (hence a slot) are not contiguous, fast fading is drawn independently for every subcarrier of a slot (Fig.2). On the other hand, the subcarriers in an AMC slot are contiguous and hence their fast fading factor can no longer be considered independent and a correlation factor of $0.5$ has been considered in simulations. Coherence bandwidth is calculated by taking into account the powers and delays of six paths of Vehicular-A profile with speed of MS equal to $60$ Kmph (Tab. A.1.1 of [10]) and is found to be $1.12$ MHz.

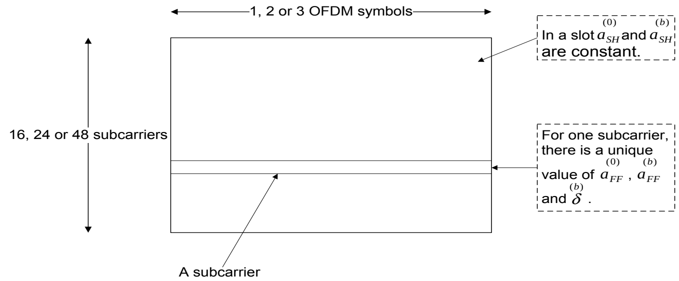


Fig. 2. Shadowing and fast fading over a PUSC/FUSC/AMC slot.

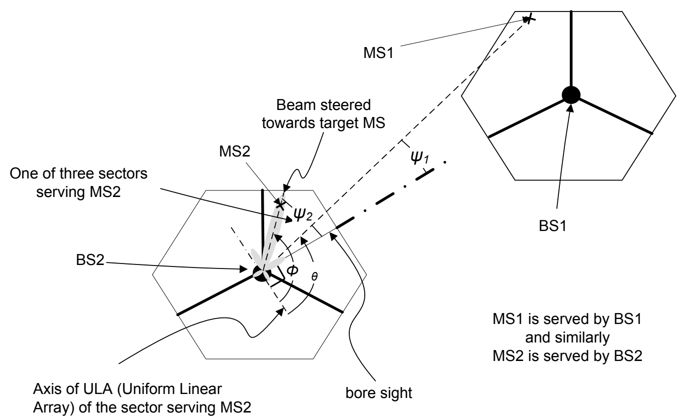


Fig. 3. Example showing beamforming scenario

### C. Beamforming Model

The beamforming model considered in our simulation is the delay and sum beamformer (or conventional beamformer) with uniform linear array (ULA). The power radiation pattern for a conventional beamformer is a product of array factor and radiation pattern of a single antenna. The array factor for this power radiation pattern is given as [14]:

$$AF(\theta) = \frac{1}{n_t} \left| \frac{\sin(\frac{n_t \pi}{2}(\cos(\theta) - \cos(\phi)))}{\sin(\frac{\pi}{2}(\cos(\theta) - \cos(\phi)))} \right|^2, \quad (2)$$

where $n_t$ is the number of transmit antennas at BS (with inter-antenna spacing equal to half wavelength), $\phi$ is the look direction (towards which the beam is steered) and $\theta$ is any arbitrary direction. Both these angles are measured with respect to array axis at BS (see Fig.3).

The gain of single antenna associated with array factor is given by Eq.3 [10]:

$$G(\psi) = G_{max} + \max\left[-12\left(\frac{\psi}{\psi_{3dB}}\right)^2, -G_{FB}\right], \quad (3)$$

where $G_{max}$ is the maximum antenna gain in boresight direction, $\psi$ is the angle MS subtends with sector boresight such that $|\psi| \leq 180°$, $\psi_{3dB}$ is the angle associated with half power beamwidth and $G_{FB}$ is the front-to-back power ratio.

### D. Path Loss Model

Line-of-sight (LOS) path loss ($PL$) model for suburban macro (scenario C1) has been referred from [13]. It is a three slope model described by following expressions:

$$PL(d) = \begin{cases} free\ space\ model & \text{if } d \le 20m; \\ C(f_c) + 23.8log_{10}(d) & \text{if } 20m < d \le d_{BP}; \\ C(f_c) + 40log_{10}(d/d_{BP}) & \text{if } d > d_{BP}, \\ +23.8log_{10}(d_{BP}) & \end{cases}$$

where $f_c$ is the carrier frequency in Hz, $C(f_c)$ is the frequency factor given as: $33.2 + 20log_{10}(f_c/2 \cdot 10^9)$, $d_{BP}$ is the breakpoint distance computed as: $4h_{BS}h_{MS}/\lambda_c$ and $\sigma_{Sh}$ is the standard deviation of log-normal shadowing. The value of $\sigma_{Sh}$ associated with above model is $4\ dB$ for $d \le d_{BP}$ and is equal to $6\ dB$ beyond $d_{BP}$.

### *E. Simulator Details*

The frequency reuse pattern considered in simulations is 1x3x1 (Fig.1). The number of cells in the network is nineteen (i.e., eighteen interfering BS). To speed up the simulation process and to include the effect of an infinite network, wraparound technique has been employed. A significant number of snapshots are being carried out for Monte Carlo simulations. Locations of MS in a sector are drawn using uniform random distribution and beams are steered according to these locations. At BS, four transmitting antennas have been considered while MS is supposed to possess one receiving antenna. All simulations are carried out with full loading of subchannels per sector.

As explained earlier, when PUSC is used, there can be up to six beams per sector i.e., one beam per group. To find the direction of adaptive beams, equivalent number of MS are drawn in a cell using spatial uniform distribution. It is to be noted that number of channels per even and odd group are different (see Tab.I). Hence, the selection of interfering beam per subcarrier is not equally probable. For a particular subcarrier, the probability of interfering with an even beam is given as:

$$p_e = \frac{N_e}{N_{Sch}},$$

and with an odd beam it is:

$$p_o = \frac{N_o}{N_{Sch}}.$$

Considering a subcarrier, six MS are drawn per interfering sector. Respective beams are steered, three of them are odd and the others three are even. In a given interfering sector, the chosen beam is drawn according to the above discrete distribution.

In case of FUSC and AMC, one MS is drawn per sector and all subcarriers of a slot experience the same interfering beam pattern from a neighboring sector.

During every snapshot, $SINR_{eff}$ of a MS is calculated using MIC model. Cell space around BS is divided into twenty rings. Since MS is dropped using uniform random distribution, during a snapshot, it might be located in any of the twenty rings. $SINR_{eff}$ and throughput are averaged over each of these rings and over complete cell as well. The former is used to study the effect of change in the values of $SINR_{eff}$ and throughput w.r.t. distance from the BS. If $SINR_{eff}$ value of a MS during a snapshot is less than 2.9 dB (threshold value being referred from [15]), it is considered to be in outage. Throughput of a MS during a snapshot, depends upon the MCS used by it.

TABLE II
PARAMETERS OF SIMULATIONS [10].

| Parameter | Value |
|---|---|
| Carrier frequency $f_c$ | 2.5 GHz |
| BS rms tansmit power $P_{Tx}$ | 43 dBm |
| Subcarrier spacing $\triangle f$ | 10.9375 kHz |
| No. of DL OFDM Symbols $N_S$ | 30 |
| Thermal noise density $N_0$ | -174 dBm/Hz |
| One side of hexagonal cell $R$ | 1.5 Km |
| Height of BS $h_{BS}$ | 32 m |
| Height of MS $h_{MS}$ | 1.5 m |
| Antenna Gain (boresight) $G_{max}$ | 16 dBi |
| Front-to-back power ratio $G_{FB}$ | 25 dB |
| 3-dB beamwidth $\psi_{3dB}$ | 70° |
| No. of transmitting antennas per sector for beamforming $n_t$ | 4 |

Simulation parameters are given in Tab.II. The parameter values are mainly based on [10].

## V. SIMULATION RESULTS

In this section, we present simulation results. In Fig. 4, average values of effective SINR ($SINR_{eff}$) are plotted as a function of distance from base station (BS). As can be noticed, there is almost no difference between values of $SINR_{eff}$ with PUSC, FUSC and AMC when it is average at a given distance. On the other hand, when we look at MCS probabilities in Fig. 5, PUSC outclasses the other two (FUSC and AMC) in terms of outage probabilities. Though average $SINR_{eff}$ are same for all, only PUSC offers an outage probability in acceptable range (less than 5%).

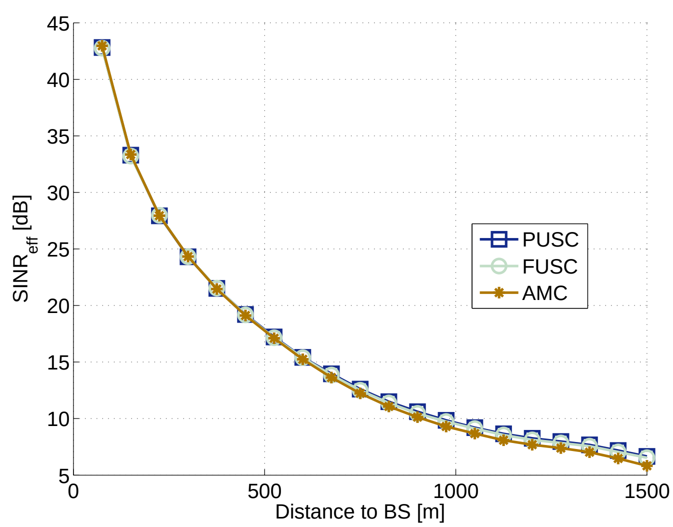


Fig. 4. Comparison of average $SINR_{eff}$ versus distance from base station with PUSC, FUSC and AMC.

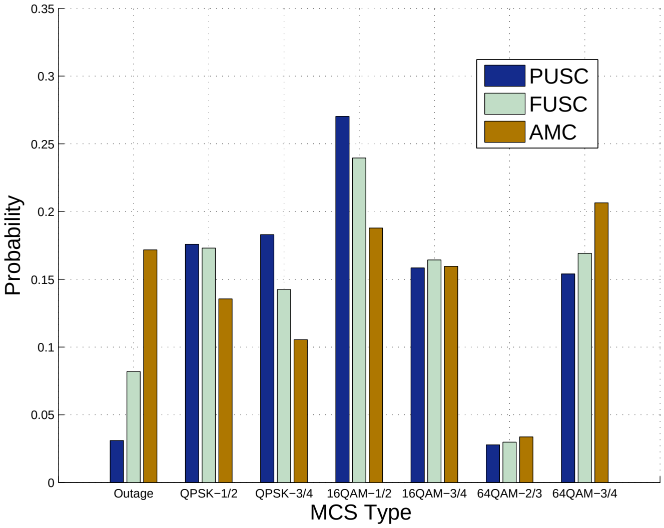


Fig. 5. Comparison of MCS probabilities with PUSC, FUSC and AMC.

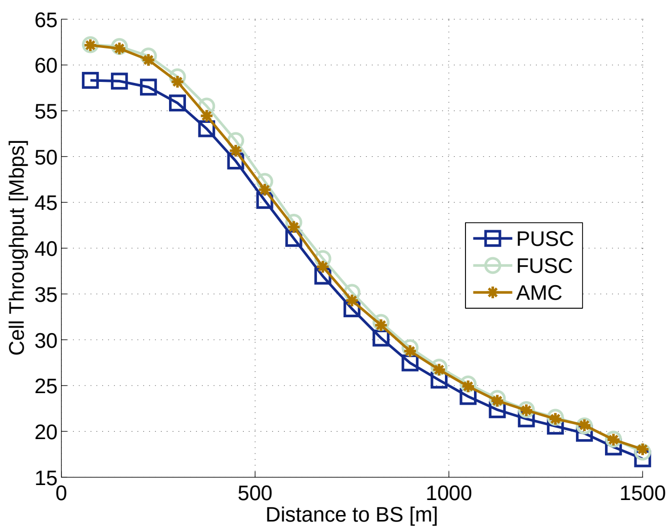


Fig. 6. Comparison of average cell throughput versus distance from base station with PUSC, FUSC and AMC.

If we look at average values of cell throughput (w.r.t. distance from BS) in Fig. 6, it can be noticed that in the region close to BS, PUSC is somewhat less performing than FUSC and AMC. This result can be justified in light of probabilities of MCS in Fig. 5 where stationary probabilities of the best MCS (64QAM-3/4) are higher with FUSC and AMC. Owing to strong signal strength in the region close to base station, probability for a MS to achieve better MCS is more. At about $350$ m and onward (from base station), throughput with PUSC is around $1$ Mbps less than that of FUSC and AMC even PUSC has better performance in terms of radio qualty. This is because of the fact that with PUSC, number of available data subcarriers are lesser and pilot subcarriers are greater than the other two.

## VI. CONCLUSION

Currently, WiMAX networks are going through trial phase. Therefore, it is important at this stage to analyze various features of WiMAX. In this paper, we have studied the possibility of adaptive beamforming in connection with three subcarrier permutation types of WiMAX. We have shown that beamforming per PUSC group offers a low outage probability as compared to FUSC and AMC. FUSC and AMC have more number of data subcarriers and hence the resultant throughput with the two is slightly more than that of PUSC. At the same time, outage probabilities for FUSC and AMC are more than 5%. Hence, adaptive beamforming per PUSC group can be exploited to achieve acceptable radio quality without need of partial loading of subchannels or base station coordination.

## REFERENCES


[1] "IEEE Standard for Local and Metropolitan Area networks, Part 16: Air Interface for Fixed and Mobile Broadband Wireless Access Systems, Amendment 2: Physical and Medium Access Control Layers for Combined Fixed and Mobile Operation in Licensed Bands and Corrigendum 1," 2005.

[2] G. Kulkarni, S. Adlakha, and M. Srivastava, "Subcarrier Allocation and Bit Loading Algorithms for OFDMA-Based Wireless Networks," in *IEEE Trans. on Mobile Computing*, December 2005.

[3] J. W. Porter, J. F. Kepler, T. P. Krauss, F. W. Vook, T. K. Blankenship, V. Desai, A. Schooler, and J. Thomas, "An Experimental Adaptive Beamforming System for the IEEE 802.16e-2005 OFDMA Downlink," in *Proc. of IEEE Radio and Wireless Symposium*, January 2007.

[4] R. Pabst, J. Ellenbeck, M. Schinnenburg, and C. Hoymann, "System Level Performance of Cellular WiMAX IEEE 802.16 with SDMA-enhanced Medium Access," in *Proc. of IEEE WCNC*, March 2007, pp. 1820–1825.

[5] M. C. Necker, "Towards Frequency Reuse 1 Cellular FDM/TDM Systems," in *ACM MSWiM*, October 2006.

[6] M. C. Necker, "Coordinated Fractional Frequency Reuse," in *ACM MSWiM*, October 2007.

[7] M. Maqbool, M. Coupechoux, and P. Godlewski, "Comparison of Various Frequency Reuse Patterns for WiMAX Networks with Adaptive Beamforming," in *Proc. of IEEE VTC Spring*, May 2008.

[8] M. Maqbool, M. Coupechoux and P. Godlewski, "Effect of Distributed Subcarrier Permutation on Adaptive Beamforming in WiMAX Networks," in *Proc. of IEEE VTC Fall*, September 2008.

[9] M. Maqbool, M. Coupechoux, and P. Godlewski, "Subcarrier Permutation (IEEE 802.16e)," TELECOM ParisTech), Technical Report, 2008.

[10] K. Ramadas and R. Jain, "WiMAX System Evaluation Methodology," Wimax Forum, Tech. Rep., January 2007.

[11] C. Lengoumbi, P. Godlewski, and P. Martins, "Subchannelization Performance for the Downlink of a Multi-Cell OFDMA System," in *Proc. of IEEE WiMob*, January 2007.

[12] "IEEE Standard for local and metropolitan area networks - Part 16: Air Interface for Fixed Broadband Wireless Access Systems," 2004.

[13] D.S. Baum et al., "IST-2003-507581, D5.4 Final Report on Link and System Level Channel Models. WINNER," October 2005, https://www.ist-winner.org/DeliverableDocuments/D5.4.pdf.

[14] D. Tse and P. Viswanath, *Fundamentals of Wireless Communications*. Cambridge University Press, 2006.

[15] "WiMAX Forum Mobile System Profile 4 Release 1.0 Approved Specification. Wimax Forum," May 2007.